Korean J. Chem. Eng., 36(10), 1716-1723 (2019)
DOI: 10.1007/s11814-019-0371-2

pISSN: 0256-1115
eISSN: 1975-7220

Enhanced performance in the photocatalytic degradation of 2,4,5-Trichlorophenoxyacetic acid over Eu-doped Bi_2WO_6 under visible light irradiation

Seong-Soo Lee*,‡, Bui The Huy*,,‡, Nguyen Thi Kim Phuong***, Do Khanh Tung****, and Yong-Ill Lee*,†**

*Department of Chemistry, Changwon National University, Changwon 51140, Korea
**Institute of Research & Development, Duy Tan University, 3 Quang Trung, Danang, Vietnam
***HoChiMinh City Institute of Resources Geography, VAST, 01 Mac Dinh Chi, Ho Chi Minh City, Vietnam
****Institute of Materials Science, VAST, 18 Hoang Quoc Viet, Cau Giay, Hanoi, Vietnam
(*Received 16 May 2019 • accepted 22 August 2019*)

Abstract−In order to make long-lived photoexcited charges for efficient catalytic photodegradation, rare earth elements are often incorporated into semiconductors. We studied the doping effect on photodegradation efficiency of Bi_2WO_6 samples with europium ions which were successfully synthesized by a simple one-step. The prepared catalyst was characterized by multiple techniques, such as X-ray diffraction (XRD), scanning electron microscopy (SEM), X-ray photoelectron spectroscopy (XPS), and UV-vis diffuse reflectance spectroscopy (DRS). The photocatalytic activities of pristine Bi_2WO_6 and *x*Eu-Bi_2WO_6 (x=1, 2, 3, and 4) were investigated in the presence of H_2O_2 for 2,4,5-Trichlorophenoxyacetic acid (2,4,5-T) as a target contaminant under visible light irradiation. The incorporation of Eu^{3+} into Bi_2WO_6 where Eu^{3+} ion played the role of an electron acceptor was favorable for transferring photoinduced electrons from Bi_2WO_6 to Eu^{3+}, thereby increasing separation efficiency of photoinduced electron-hole, leading to enhanced photocatalytic activity of *x*Eu-Bi_2WO_6. Under optimized condition, the photodegradation efficiency of 2,4,5-T by 2Eu-Bi_2WO_6 samples was 1.7-fold higher than that of pristine Bi_2WO_6 sample. We demonstrate that Eu^{3+} ion is a promising candidate for the development of a visible-light active semiconductor catalyst for environmental remediation.

Keywords: Photocatalytic, Acceptor, Herbicide, Toxicity, Visible Light

INTRODUCTION

The photocatalyst as a green chemistry technique has been applied extensively for the proficient degradation of various toxic organic compounds in the environment. Several key factors are often required for promoting photocatalytic activity, including high surface area and efficient separation of electron-hole pairs of catalysts. Semiconductor photocatalysts can utilize solar energy more efficiently in comparison with wide traditional photocatalysts, for example TiO_2 and ZnO [1]. Tungstate based materials such as Y_2WO_6 [2], $CaWO_4$ [3,4], $ZnWO_4$ [5,6], and Bi_2WO_6, have been widely investigated owing to their desirable electric and optical properties. Bi_2WO_6 as one of the Aurivillius oxides can act as a supportable photocatalyst for eliminating environmental contaminants under visible light exposure because of its low band gap (about 2.7 eV). However, the recombination of the electrons and holes in photodegradation process on Bi_2WO_6 is too rapid to achieve photocatalytic activity with high efficiency. To improve the photocatalytic capability of Bi_2WO_6 material, various attempts have been made for the synthesis of heterostructural composites and surface modification. Zhou's group decorated Au on Bi_2WO_6 surface to investigate the photocatalytic activity for removing toxic phenol compounds and chromium(VI) in aqueous solution [7]. Several other groups also prepared the heterostructure of AgBr/Bi_2WO_6, BiOCl/Bi_2WO_6, and Bi_2S_3/Bi_2WO_6 to enhance the photodegradation activity on rhodamine B and salicylic acid [8-11]. However, these approaches require complicated synthetic processes and are time consuming. As a simple method, Bi_2WO_6 is often doped by metal or non-metal elements to incorporate with other oxides [12-16]. It is known that rare earth elements have 4f and empty 5d orbitals, which are incomplete occupied orbitals, to give the increase of optical absorption of material and of the efficiency for the separation of photo-generated electron hole pairs. Therefore, Bi^{3+} with $6s^2$ electronic configuration has been expected to be a suitable sensitizer for rare earth ions [17,18]. Although the photocatalytic viability of Bi_2WO_6 has been evaluated for many types of dyes, including rhodamine B, methyl orange, and methylene blue [1,16,19,20], to the best of our knowledge, studies on the photocatalytic activity of Bi_2WO_6 for herbicides and the explanation for role of Eu^{3+} ion as an electron acceptor in photocatalytic process are still rare.

2,4,5-Trichlorophenoxy acetic acid (2,4,5-T) has been widely used as a herbicide for defoliating broad-leafed weeds. However, its high toxicity and lesser biodegradation property bring serious consequences for the environment. Therefore, the elimination or reduction of excessive 2,4,5-T have been paid much attention in recent years. Studies on photocatalytic activity photodegradation of 2,4,5-T were performed on MgFeTi layered double hydroxides [21], Fe(II)-catalyzed activation of Oxone [22], and TiO_2 [23].

Herein, we present the enhancement of photocatalytic activity of

†To whom correspondence should be addressed.
E-mail: yilee@changwon.ac.kr
‡The authors are co-first authors.

Bi_2WO_6 material for the photodegradation of 2,4,5-T by doping Eu^{3+} ions, which play the role of electron acceptor in Bi_2WO_6 host under visible light irradiation. The proposed material was prepared by a facile one-step hydrothermal method. The effects of amount of dopant, pH, stability, and available reusability were evaluated. The *x*Eu-Bi_2WO_6 samples exhibited much higher photodegradation performance compared with that of pristine Bi_2WO_6 sample. In addition, we propose a probable photodegradation mechanism as well.

EXPERIMENT

1. Synthesis

Bismuth nitrate pentahydrate ($Bi(NO_3)_3{\cdot}5H_2O$, 99.99%), sodium tungstate dihydrate ($Na_2WO_4{\cdot}2H_2O$, 99%), europium(III) nitrate pentahydrate ($Eu(NO_3)_3{\cdot}5H_2O$, 99.9%), and 2,4,5-Trichlorophenoxyacetic acid were purchased from Sigma-Aldrich (USA). All chemicals were used without further purification. Deionized water (DW) was used in all experiments. For preparing Eu-doped Bi_2WO_6 samples, $Bi(NO_3)_3{\cdot}5H_2O$ (2 mmol) was dissolved in 180 mL DW using a water sonicator bath at 40 °C for one hour. Specific amounts of Eu^{3+} were added into the above solution under stirring. The tungstate source from $Na_2WO_4{\cdot}2H_2O$ (1 mmol) in 20 mL DW was delivered to the mixture solution by using a syringe pump with the speed of 2 mL/min. The mixture was stirred for two hours and transferred into Teflon-line autoclaves to heat at 200 °C for 20 h. For clarification, the synthesized samples are denoted as *x*Eu-Bi_2WO_6; herein, *x* represents the percentage of Eu in the as-prepared samples. Hereafter this is referred to as pristine Bi_2WO_6, *1*Eu-Bi_2WO_6, *2*Eu-Bi_2WO_6, *3*Eu-Bi_2WO_6 and *4*Eu-Bi_2WO_6. The precipitate was collected and washed several times by centrifugation. The product was obtained after drying for overnight at 50 °C.

2. Characterization

Crystalline study of the prepared samples was analyzed by X-ray powder diffraction using an X-ray diffractometer X'Pert PW3030/00 from PANalytical (Almelo, Netherlands) with Cu-K_α radiation. Field emission scanning electron microscope (FE-SEM) images were obtained at an operating voltage of 20 kV (MIRE-II Tescan, Czech Republic). The 2,4,5-T concentration was determined by using an UV-Visible spectrophotometer (Thermo Evolution 201, US). The absorption spectra of the samples were recorded using diffuse reflectance spectroscopy (DRS) (V-670, Jasco, Japan). X-ray photoelectron spectra (XPS) of the prepared sample were recorded on a K-Alpha X-ray photoelectron spectrometer system (Thermo Scientific).

3. Photocatalytic Experiments

The photodegradation activities of the samples were examined based on the degradation reaction of 2,4,5-T under visible light generated by simulated AM 1.5G sunlight system. The temperature of the reactor was kept at 15 °C using a circulating water system. In all experiments, 100 mg of catalyst was dispersed in a 100 mL of 2,4,5-T solution (100 mg/L). First step, the suspension was stirred in a dark box for 60 min to get an equilibrium between the

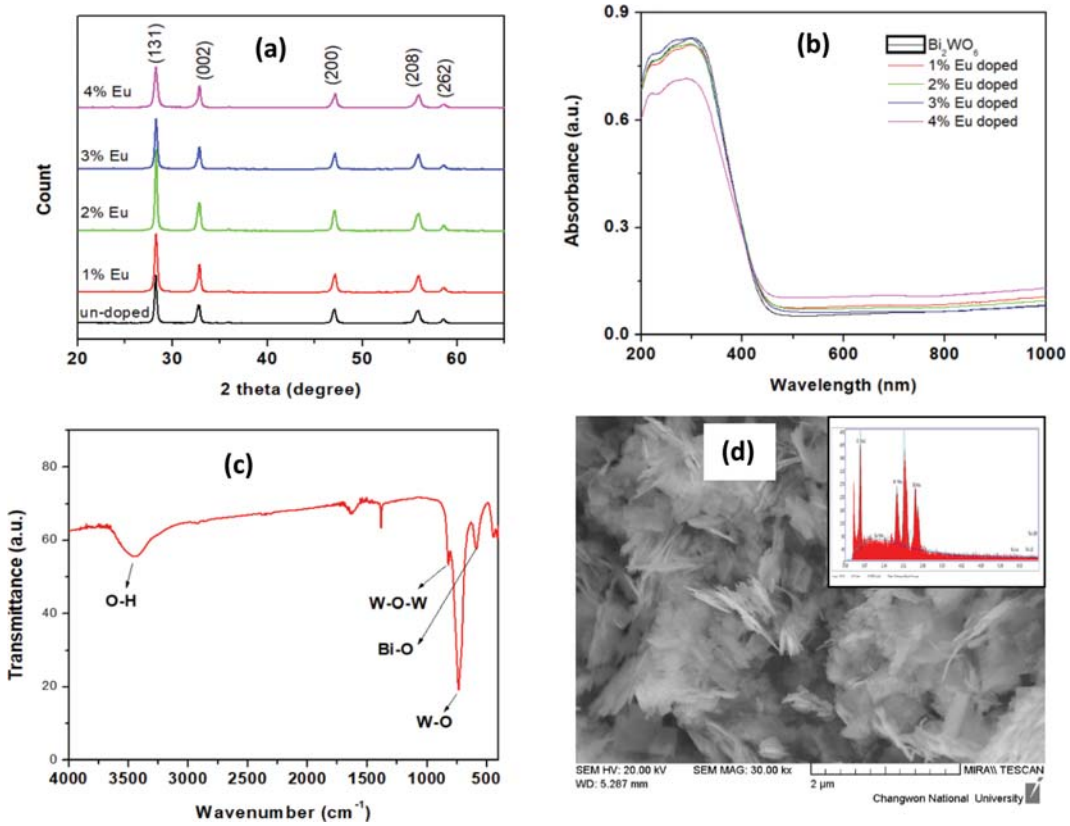

Fig. 1. (a) XRD patterns of *x*Eu-Bi_2WO_6 samples, (b) UV-Vis diffuse reflectance spectra *x*Eu-Bi_2WO_6 samples, (c) FT-IR spectrum of *2*Eu-Bi_2WO_6 sample, and (d) SEM image of the *2*Eu-Bi_2WO_6.

Table 1. The lattice parameters of the prepared samples from Rietveld refinement analysis

	Pristine Bi_2WO_6	*1*Eu-Bi_2WO_6	*2*Eu-Bi_2WO_6	*3*Eu-Bi_2WO_6	*4*Eu-Bi_2WO_6
a (Å)	5.438	5.440	5.438	5.437	5.443
b (Å)	16.446	16.440	16.443	16.442	16.448
c (Å)	5.445	5.443	5.441	5.442	5.433
V/ 10^6 pm^3	486.895	486.735	486.529	486.488	486.409
Crystallite size (nm)	48	45	44	40	31

adsorption and desorption process of the catalyst and 2,4,5-T. Subsequently, the suspension was irradiated with a Xenon lamp. To assess the efficiency of the degradation reaction in the H_2O_2-Vis light system, small amounts of H_2O_2 were added to the mixture of 2,4,5-T and catalyst. Five milliliter suspension was sampled at different time intervals and immediately centrifuged to separate the catalyst. The supernatant was quantized through the UV-Vis absorption spectra at fixed wavelength of 290 nm (absorption peak of 2,4,5-T). The photocatalytic experiments were performed in triplicate.

RESULTS AND DISCUSSION

1. Morphology Studies

The XRD patterns of the prepared samples are shown in Fig. 1(a). The diffraction peaks at 28.4°, 33.0°, 47.2°, 55.9°, and 58.7° can be identified perfectly to (131), (002), (200), (208), and (262) crystal planes of orthorhombic bismuth tungstate with space group of Pca21 (JCPDS No. 79-2381), respectively. Peaks related to Eu^{3+} were not observed in all samples to indicate a single orthorhombic phase of *x*Eu-Bi_2WO_6. It is known that ionic radii of Bi^{3+} and Eu^{3+} for the coordination number of 6 are 1.03 Å and 0.95 Å, respectively. Therefore, this small difference of ionic radii is anticipated to result in the replacement of Bi^{3+} ions by Eu^{3+} ions. The results from Rietveld refinement analysis on XRD patters with R(Bragg)<3.7% confirmed that the lattice parameters, such as unit cell dimension, volume, and crystallite size, were changed with doping Eu^{3+} ions, as presented in Table 1. The enlargement of XRD patterns (Fig. S1) shows that the diffraction peak positions of Eu-doped Bi_2WO_6 samples were slightly shifted to larger 2θ values compared with that of Eu-undoped sample. The shifts could have originated from the replacement of Bi^{3+} ions, which has larger ionic radius, to smaller Eu^{3+} ions to decrease the lattice constants [18,20].

Fig. 1(b) displays the UV-vis diffuse reflectance spectra of the prepared samples in the wavelength range of 200-1,000 nm. The absorption edge about 460 nm was observed in all samples; however, the absorbance in visible region was a little increased for Eu-doped samples. Fig. 1(c) shows the FT-IR spectrum of Eu-doped Bi_2WO_6 sample. The broad band at 3,300-3,500 cm^{-1} is attributed to the O-H stretching of adsorbed water [24,25]. The weak band at 823 cm^{-1} is assigned to the bending vibration of W-O-W. The strong band located at 734 cm^{-1} is attributed to the W-O vibration

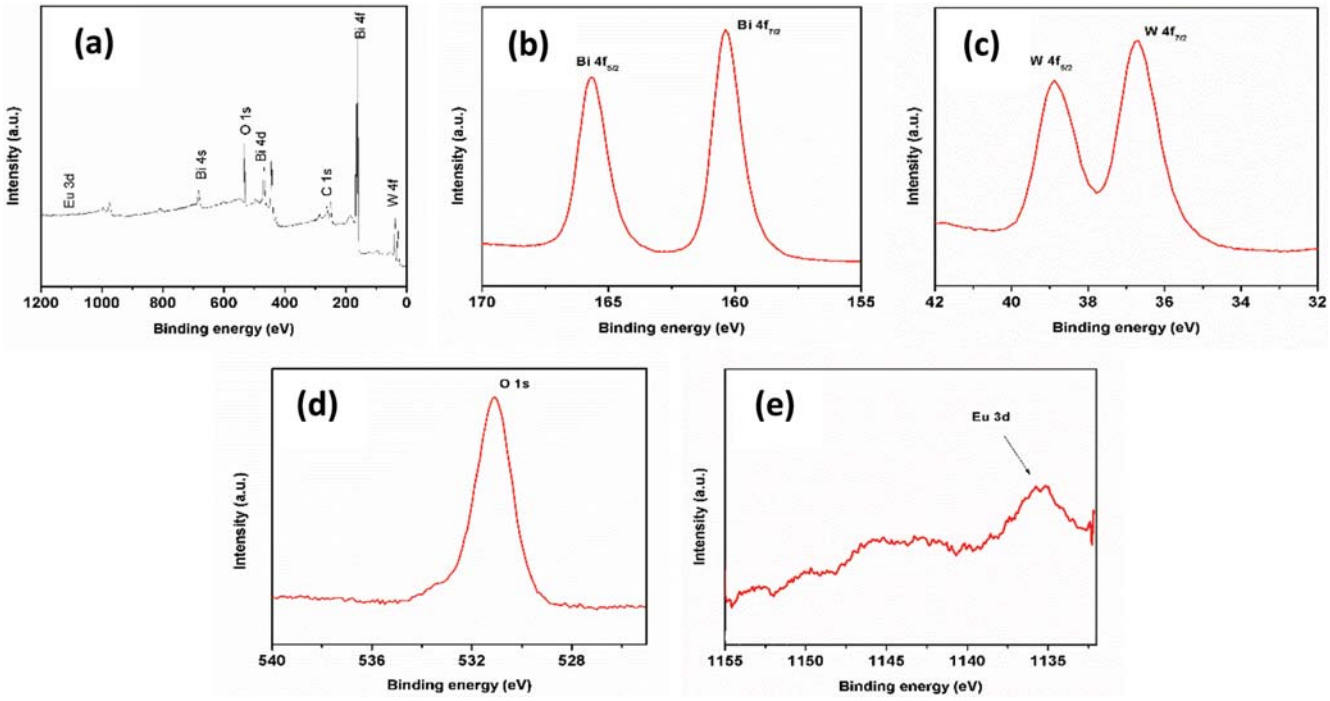

Fig. 2. XPS spectra of 2Eu-doped Bi_2WO_6 sample: (a) survey spectrum, (b) Bi 4f, (c) W 4f, (d) O 1s, and (e) Eu 3d.

in WO_6 octahedrons. The weak bands at 582 and 443 cm^{-1} are related to the Bi-O vibration of BiO_6 octahedrons. The SEM image of 2Eu-Bi_2WO_6 sample is presented in Fig. 1(d) to show the prepared sample possessing the sheet shape. The EDS result confirms the existence of Bi, W, and Eu in Eu-Bi_2WO_6 samples (inset of Fig. 1(d)). The SEM images of other samples are presented in Fig. S2. The SEM image of un-doped Bi_2WO_6 sample shows that un-doped Bi_2WO_6 sample involves irregular shapes (Fig. S1(a)). The shape of Bi_2WO_6 samples was changed to petal-like, which have different sizes, with increasing the concentration of Eu^{3+} (Fig. S2(b)-S2(e)). This change could be originating from the difference of lattice parameters, which affected growth of particles. These results also agree with a previous report [20].

The chemical composition of the prepared sample was analyzed by XPS study, focusing in particular on the band shape of Bi, W, and O. Full scan XPS spectrum of Eu-doped Bi_2WO_6 consists of the main elements of Bi, W, O, and Eu, as shown in Fig. 2(a).

High resolution XPS spectra of Bi 4f, W 4f, O 1s, and Eu 3d presented in Fig. 2(b)-(e) were calibrated with C1s, the binding energy of which is 285.8 eV. Two strong peaks at 165.6 and 160.4 eV (Fig. 2(b)) are assigned to spin-orbit splitting of Bi $4f_{5/2}$ and Bi $4f_{7/2}$, respectively [26]. The peaks located at 38.5 and 36.4 eV are from W $4f_{5/2}$ and W $4f_{7/2}$ of W^{6+}, respectively (Fig. 2(c)). In Fig. 2(d), the peak at 531.9 is related to the oxygen in Bi_2WO_6 structure in the forms of Bi-O (in $Bi_2O_2^{2+}$ slabs) and W-O bonds [27]. The Eu^{3+} ion concentration in the sample was low (2%): therefore, the signal of Eu 3d at 1,135 eV is not strong enough (Fig. 2(e)).

2. Effect of Eu^{3+} Concentration in Bi_2WO_6 for the Degradation of 2,4,5-T

The photocatalytic oxidation of 2,4,5-T was under visible light irradiation in the presence of H_2O_2. To understand the function of Eu^{3+} in the photocatalytic 2,4,5-T oxidation reaction, the photocatalytic activities of pristine Bi_2WO_6 and *x*Eu-Bi_2WO_6 (*x*=1, 2, 3, and 4%) with different duration of time were examined. Fig. 3(a) demonstrates the time dependence for the degradation of 2,4,5-T. In Fig. 3(a), the equilibrium between absorption and desorption was established for 1 h in dark; approximately 9.0-20.4% of 2,4,5-T was adsorbed on the pristine Bi_2WO_6 and *x*Eu-Bi_2WO_6 samples. This difference can originate from different shapes of the samples, which is mentioned in section of 3.1. As shown in Fig. 3(a), control experiments with H_2O_2 only showed almost no oxidation ability for 2,4,5-T under lighting or dark condition. After 6 h visible light irradiation, approximately 31.0 and 44.4% of 2,4,5-T was degraded in the presence of pristine Bi_2WO_6 and *2*Eu-Bi_2WO_6, respectively. However, the elimination of 2,4,5-T was significantly increased in simultaneous presence of catalysts (pristine Bi_2WO_6 or *x*Eu-Bi_2WO_6), H_2O_2 and visible light. As seen in Fig. 3(a), after lighting for 6 h in the presence of H_2O_2, the removal of 2,4,5-T (100 mg/L) by *2*Eu-Bi_2WO_6 catalyst reached ~82.4% followed by *1*Eu-Bi_2WO_6 (~80.4%), *3*Eu-Bi_2WO_6 (~69.5%), *4*Eu-Bi_2WO_6 (~68.7%) and Bi_2WO_6 (~47.9%). The elimination of 2,4,5-T was greater for *x*Eu-Bi_2WO_6/H_2O_2/Vis system than for pristine Bi_2WO_6/H_2O_2/Vis system to indicate that the Eu^{3+} loading on Bi_2WO_6 significantly enhanced the photocatalytic activity of *x*Eu-Bi_2WO_6. To dope Eu^{3+} into Bi_2WO_6 may improve the transfer rate of photoinduced electrons, resulting in suppressed recombination of photoinduced electrons and holes, thereby enhancing the photocatalytic activity of the *x*Eu-Bi_2WO_6 samples. *2*Eu-Bi_2WO_6 sample exhibited the highest photocatalytic activity compared with *1*Eu-Bi_2WO_6, *3*Eu-Bi_2WO_6 and *4*Eu-Bi_2WO_6 samples. This probably indicates the *1*Eu-Bi_2WO_6 sample may not produce enough free active radicals due to the deficiency of Eu^{3+}, whereas, the *3*Eu-Bi_2WO_6 and *4*Eu-Bi_2WO_6 samples provide the excessive Eu^{3+}. It might prevent Bi_2WO_6 from exposure to visible light; therefore, the separation of the photo-induced e^- and h^+ pairs of Bi_2WO_6 was limited, which reduced the catalytic activity. Therefore, controlling the Eu^{3+} content is the most important factor to improve the photocatalytic activity of *x*Eu-Bi_2WO_6 samples. Results of this study demonstrate that *x*Eu-Bi_2WO_6 catalysts or H_2O_2 when used alone, the ability to oxidize 2,4,5-T is very weak under visible light irradiation.

To clarify the degradation/mineralization of 2,4,5-T on *2*Eu-Bi_2WO_6/H_2O_2/Vis system, the amounts of total organic carbon (TOC) in solution and *2*Eu-Bi_2WO_6 catalyst were determined at initial, before, and after visible light irradiation, as display in Table 2. Note that the total removal of 2,4,5-T on *2*Eu-Bi_2WO_6/H_2O_2/Vis system was 82.4%, whereas TOC removal reached 78.46% after lighting for 6 h to confirm the excellent degradation/mineralization performance of this system. The difference of the amounts of TOC

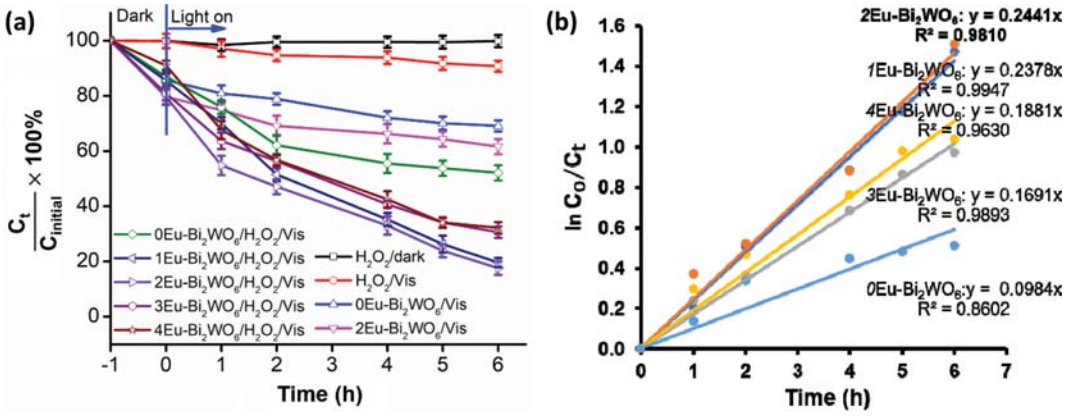

Fig. 3. Photodegradation of 2,4,5-T: (a) Effect of Eu^{3+} quantity in *x*Eu-Bi_2WO_6 samples on the photocatalytic activity and (b) Linear kinetic degradation of 2,4,5-T on *x*Eu-Bi_2WO_6/H_2O_2/Vis systems.

Table 2. Quantity of TOC in solution and on *2*Eu-Bi_2WO_6 (reaction condition: 100 mL of 2,4,5-T solution (100 mg/L), 0.1 g catalyst, pH 2.2)

		2,4,5-T (mg)	2,4,5-T (%)	TOC (mg)	TOC (%)
Solution	At initial	10.0±0.03	100.00	3.76±0.02	100.00
	Before Vis irradiation	7.96±0.03	79.60	2.95±0.03	78.46
	After Vis irradiation	1.76±0.02	**17.60**	0.71±0.05	**18.89**
*2*Eu-Bi_2WO_6	Before Vis irradiation	-	-	0.80±0.04	21.28
	After Vis irradiation	-	-	0.10±0.005	**2.66**
Remaining		1.76	17.60	0.81	21.54
Total removal		8.24	**82.40**	2.95	**78.46**

Table 3. Chloroorganics remaining in solution after the degradation process in *2*Eu-Bi_2WO_6/H_2O_2/Vis system (reaction condition: 100 mL 2,4,5-T 100 mg/L, 0.1 g catalyst, pH 2.2)

Chloroorganics calculated (mg)	Inorganic chloride in solution after 6 h of reaction (mg)	%	% Chloroorganics remaining
4.168	3.43 ± 0.04	82.29	17.71

adsorbed on *2*Eu-Bi_2WO_6 before and after visible light irradiation indicated that desorption occurred during the degradation process. Although about 0.80 mg/L of TOC (~21.28%) was adsorbed by *2*Eu-Bi_2WO_6 before the suspension was exposed by visible light, only ~0.1 mg/L of TOC (~2.66%) remained on *2*Eu-Bi_2WO_6 after lighting for 6 h (Table 2).

The degree of dechlorination from 2,4,5-T was evaluated by measuring the concentration of inorganic chloride in solution after 6 h irradiation by using a Metrohm 940 Professional Vario ion chromatography (Switzerland), and the results are presented in Table 3. Approximately 82.29% of inorganic chloride was formed after the reaction, which indicates very high efficiency of dechlorination from 2,4,5-T in *2*Eu-Bi_2WO_6/H_2O_2/Vis system.

Based on the results: 82.4% degradation of 2,4,5-T, 78.46% re-

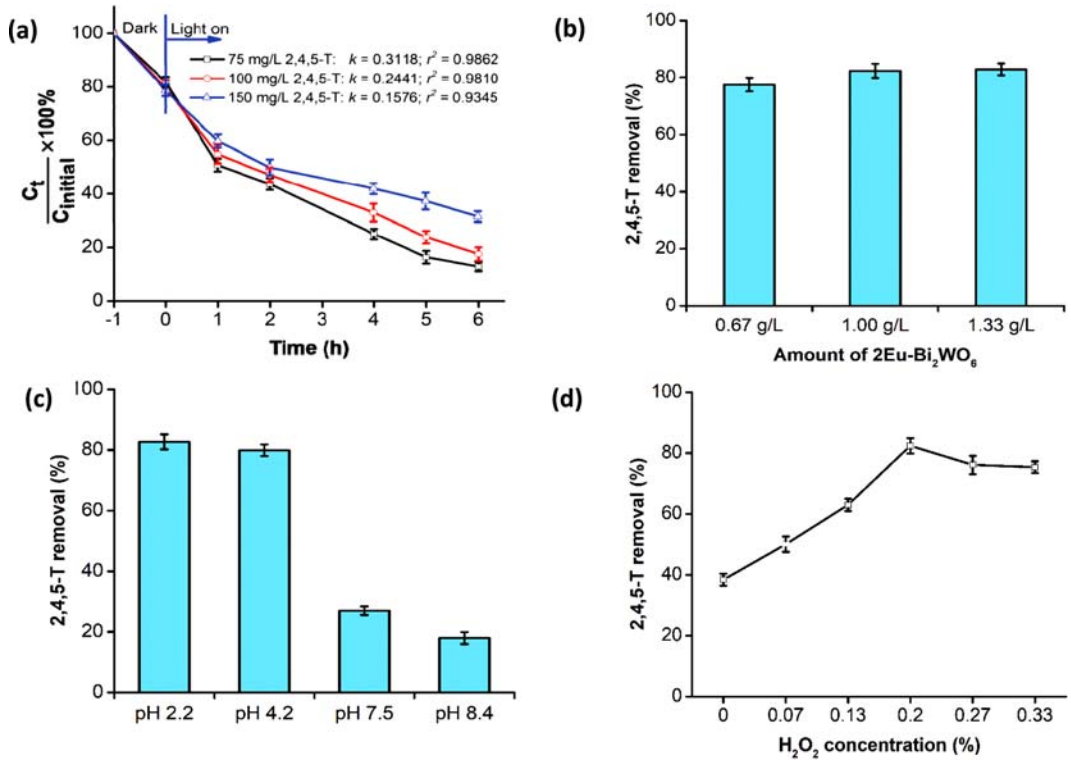

Fig. 4. Degradation of 2,4,5-T after 1 h dark adsorption following 6 h visible light irradiation (a) Effect of 2,4,5-T concentration (1.0 g/L of *2*Eu-Bi_2WO_6 sample and 0.2% of H_2O_2 30% at pH 2.2); (b) Effect of the quantity of *2*Eu-Bi_2WO_6 sample (0.2% of H_2O_2 30% and 100 mg/L 2,4,5-T at pH 2.2); (c) Effect of pH in solution (0.2% of H_2O_2 30%; 100 mg/L 2,4,5-T and 1.0 g/L of *2*Eu-Bi_2WO_6 sample) and (d) Effect of H_2O_2 concentration (1.0 g/L of *2*Eu-Bi_2WO_6 sample and 100 mg/L 2,4,5-T at pH 2.2).

moval of total organic carbon (TOC) and 82.29% generation of inorganic chloride over *2*Eu-Bi_2WO_6/H_2O_2/Vis system after 6 h of visible light irradiation, it can be concluded that 78.46% of 2,4,5-T was completely mineralized to CO_2, H_2O and inorganic chloride. About 3.83% 2,4,5-T had been dechlorinated from the benzene ring.

A typical first-order kinetic model was used to analyze the experimental data and calculate the degradation rate of 2,4,5-T. This model can be expressed by $\ln(C_0/C_t)=kt$, where t refers to reaction time (h), k is the apparent rate constant (h^{-1}), and C_0 and C_t are the concentrations (mg/L) of 2,4,5-T at time t=0 and t=t, respectively. The linear kinetic degradation and rate constants, k of 2,4,5-T on the xEu-Bi_2WO_6/H_2O_2/light systems are given in Fig. 3(b).

3. Effect of the Concentrations of 2,4,5-T and H_2O_2, the Quantity of 2Eu-Bi_2WO_6 Sample, and pH Value on the Photocatalytic Activity

Fig. 4(a) presents the influence of initial concentration of 2,4,5-T on degradation efficiency on *2*Eu-Bi_2WO_6/H_2O_2/Vis light system. The photocatalytic efficiency decreased with increasing the initial concentration of 2,4,5-T. Increasing the concentration of 2,4,5-T from 75 to 150 mg/L is associated with decreasing the degradation efficiency of 2,4,5-T from 87.04% to 68.47% at 6 h. The influence of the amount of the catalyst on the photodegradation efficiency 2,4,5-T (100 mg/L) was studied after 6 h reaction using different amount of the catalyst (see Fig. 4(b)). It was observed that the 2,4,5-T degradation efficiency increased with the increase of the amount of the *2*Eu-Bi_2WO_6 from 0 to 1.0 g/L. However, the degradation efficiency of 2,4,5-T did not increase with subsequent increase in *2*Eu-Bi_2WO_6 beyond 1.0 g/L. Excessive amount of *2*Eu-Bi_2WO_6 catalyst resulted in highly turbid solutions causing a shield-reflection effect from light which reduced the number of photons to interact with *2*Eu-Bi_2WO_6 catalyst.

In the photocatalytic reactions, the pH value of the solution is an important factor. A satisfactory explanation of the pH effect is not easy because there are many factors that appear in this process, such as electrostatic interaction between the catalyst surface and the pollutants, the ionization state of the surface of the catalyst, and generated charged radicals. The pH dependence of photodegradation of 2,4,5-T on *2*Eu-Bi_2WO_6/H_2O_2/Vis light system was investigated. We found that 2,4,5-T degradation decreased with increasing pH in the solution from 2.2 to 8.4, as shown in Fig. 4(c). At low pH, the surface of the *2*Eu-Bi_2WO_6 catalyst can be protonated leading to increasing electrostatic interactions between the *2*Eu-Bi_2WO_6 surface (positive charge) and the 2,4,5-T (negative charge) [28,29].

Fig. 4(d) shows the photodegradation efficiency for 2,4,5-T on the *2*Eu-Bi_2WO_6/Vis system in the presence of various concentrations of H_2O_2 at pH 2.2. Interestingly, the photodegradation of 2,4,5-T significantly increased by increasing the amount of H_2O_2 (from 0 to 0.2%). Approximately 82.4% of the 2,4,5-T was degraded on 2Eu-Bi_2WO_6/H_2O_2/Vis system using 0.2% H_2O_2 solution within 6 h.

H_2O_2 mainly acts as an electron scavenger and generates hydroxyl radicals (OH•) simultaneously [30]:

$$H_2O_2+e^- \rightarrow OH^{\bullet}+OH^- \quad (1)$$

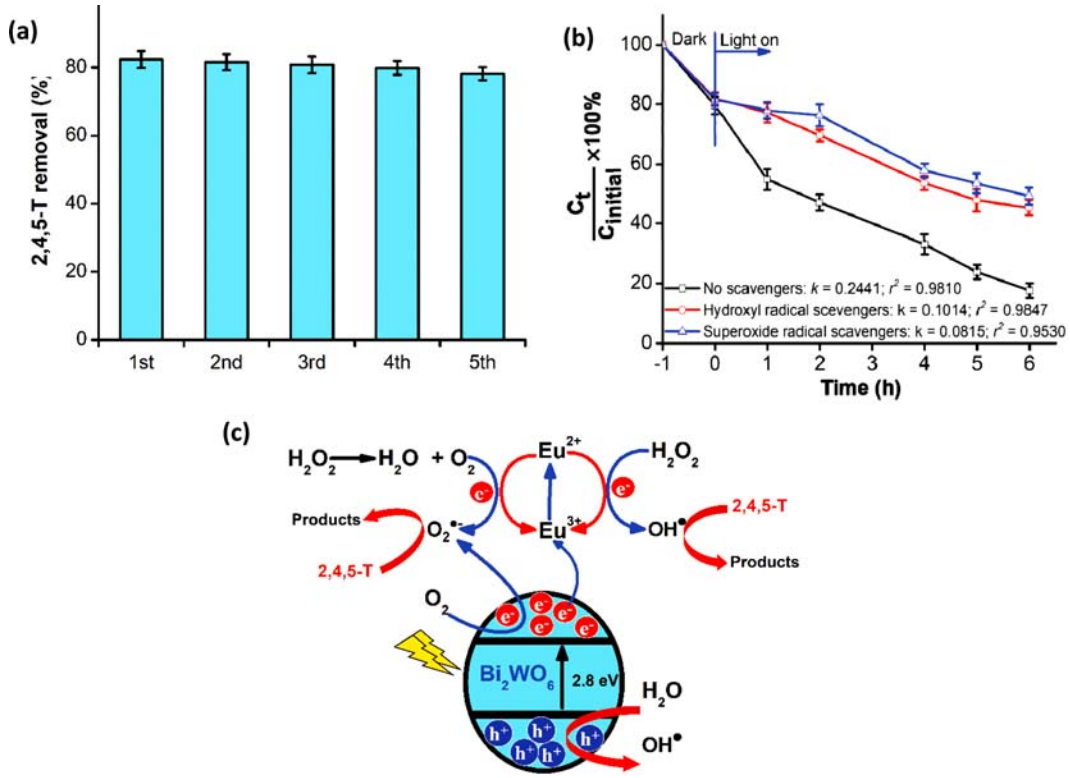

Fig. 5. (a) Reusability of catalyst on 2,4,5-T photodegradation over *2*Eu-Bi_2WO_6/H_2O_2/Vis system (b) The rate constant, k for the photodegradation of 2,4,5-T on *2*Eu-Bi_2WO_6/H_2O_2/Vis system with the addition of $O_2^{\bullet-}$ and OH• radical scavengers and (c) The proposed mechanisms of 2,4,5-T photodegradation on *2*Eu-Bi_2WO_6/H_2O_2/Vis system.

However, beyond adding 0.2% of H_2O_2, the efficiency of 2,4,5-T was decreased, presumably due to excessive amount of H_2O_2 acting as an OH radical scavenger. The generated $OH^{\bullet}$ radicals may react with excessive H_2O_2 to form hydroperoxyl radicals ($OOH^{\bullet}$). The oxidation potential for OOH is much lower than that for $OH^{\bullet}$ to decrease the free available radicals for 2,4,5-T oxidation, leading to low degradation efficiency [31,32]:

$$H_2O_2+OH^{\bullet}\rightarrow H_2O+OOH^{\bullet} \quad (2)$$

4. Reusability and Mechanism

The practical application of a photocatalyst requires its stability; therefore, the *2*Eu-Bi_2WO_6 sample was evaluated for stability and reusability. The reuse stability of the catalyst over *2*Eu-BiW_2O_6/H_2O_2/Vis system on the 2,4,5-T degradation was carried out with an initial 2,4,5-T concentration of 100 mg/L, at pH 2.2 with a solid/liquid ratio of 0.1 g/L and 0.2% H_2O_2 concentration. After 1 h of dark adsorption and 6 h of visible light irradiation, the catalyst was separated by centrifugation and then added to fresh solution of 2,4,5-T. The process was repeated five times. The results in Fig. 5(a) show that the photocatalytic performance of *2*Eu-Bi_2WO_6 in the *2*Eu-BiW_2O_6/H_2O_2/Vis system is highly recyclable with only negligible decrease (~4%) after five cycles.

To understand the involvement of free active radical species in the degradation of 2,4,5-T on the *2*Eu-Bi_2WO_6/H_2O_2/Vis light systems, ethanol as an $OH^{\bullet}$ radical scavenger and ascorbic acid as a superoxide anion ($O_2^{\bullet-}$) radical scavenger were added separately to the system. It was obvious that the addition of ethanol to the *2*Eu-Bi_2WO_6/H_2O_2/Vis system, the degradation efficiency of 2,4,5-T was decreased remarkably, as shown in Fig. 5(b). Only 55% of 2,4,5-T was degraded on *2*Eu-Bi_2WO_6/H_2O_2/Vis system without $OH^{\bullet}$ radicals after lighting for 6 hrs, indicating the strong contribution of $OH^{\bullet}$ radicals. As seen in Fig. 5(b), the rate constant (k) for the degradation of 2,4,5-T on *2*Eu-Bi_2WO_6/H_2O_2/Vis system was reduced from 0.2441 min^{-1} to 0.1014 min^{-1} when OH radical was removed (decreased 2.4-fold). In addition, a large suppression of 2,4,5-T degradation was noted upon the addition of ascorbic acid to the *2*Eu-Bi_2WO_6/H_2O_2/Vis system. The degradation of 2,4,5-T was reduced from 82.8% to 50.7%, as such, O_2^{-} radicals also served as the major active species in this system. After lighting for 6 hrs, the rate constant of 2,4,5-T degradation on *2*Eu-Bi_2WO_6/H_2O_2/Vis system radicals was 0.0815 min^{-1} in the absence of $O_2^{\bullet-}$. The result suggests that both $OH^{\bullet}$ and $O_2^{\bullet-}$ radicals are major oxidizing species for the degradation of 2,4,5-T on *2*Eu-Bi_2WO_6/H_2O_2/Vis system.

From a photocatalytic point of view, we propose a mechanism for photodegradation of 2,4,5-T using Eu-doped Bi_2WO_6 in this work. As illustrated in Fig. 5(c), Bi_2WO_6 in *2*Eu-Bi_2WO_6 was first excited and produced photo-induced e^{-}-h^{+} pairs under visible light irradiation. Once photo-induced e^{-} is generated, they jumped quickly over Eu^{3+} ion to form Eu^{2+}, as such, Eu^{3+} acts as an electron acceptor center [18]. The generated Eu^{2+} can react either with H_2O_2 to produce $OH^{\bullet}$ radicals or with O_2 to produce $O_2^{\bullet-}$ radicals and reverts to the original state Eu^{3+}. The enhancement of the photocatalytic activity of *2*Eu-Bi_2WO_6 is due to the photo-induced e^{-} of Bi_2WO_6 captured further quickly by Eu^{3+} ions, thus preventing the recombination of the photo-induced e^{-}-h^{+}. In addition, the photo-induced h^{+} can react with H_2O to generate $OH^{\bullet}$ radicals as well as photo-induced e^{-} can react directly with O_2 to generate $O_2^{\bullet-}$ radicals. The generated $OH^{\bullet}$ and $O_2^{\bullet-}$ radicals oxidize 2,4,5-T rapidly to CO_2 and water as degradation products.

The mechanism of 2,4,5-T degradation on *2*Eu-Bi_2WO_6/H_2O_2/Vis system can be described by the following reactions:

$$Bi_2WO_6+h\nu\rightarrow Bi_2WO_6\ (e_{CB^-}, h_{VB^+}) \quad (3)$$

$$Eu^{3+}+e_{CB^-}\rightarrow Eu^{2+}\ (\text{Major reaction}) \quad (4)$$

$$Eu^{2+}+H_2O_2\rightarrow Eu^{3+}+OH^{\bullet}+OH^{-} \quad (5)$$

$$h_{VB^+}+2H_2O\rightarrow OH^{\bullet}+H^{+} \quad (6)$$

$$2H_2O_2\rightarrow O_2+2H_2O \quad (7)$$

$$Eu^{2+}+O_2\rightarrow Eu^{3+}+O_2^{\bullet-} \quad (8)$$

$$O_2^{\bullet-}+2,4,5\text{-T}\rightarrow\text{degradation products} \quad (9)$$

$$OH^{\bullet}+2,4,5\text{-T}\rightarrow\text{degradation products} \quad (10)$$

CONCLUSION

Eu-doped Bi_2WO_6 samples were prepared by a facile one-step hydrothermal method, and the photodegradation efficiency for 2,4,5-T was investigated under visible light. *2*Eu-Bi_2WO_6 catalyst exhibited very high photocatalytic activity for the degradation of 2,4,5-T with the degradation rate of 0.2441 min^{-1} in the presence of H_2O_2. Eu^{3+} ions played thte role of electron acceptors and were favorable for transferring photoinduced electrons from Bi_2WO_6 to Eu^{3+} to result in separation efficiency of photoinduced electron-holes. The mineralization of 2,4,5-T on *2*Eu-Bi_2WO_6/H_2O_2/Vis light system was confirmed by measuring TOC values. The addition of radical scavengers demonstrates that the $OH^{\bullet}$ and $O_2^{\bullet-}$ radicals are the main active species for 2,4,5-T degradation on *2*Eu-Bi_2WO_6/H_2O_2/Vis system. The synergetic effect of Bi_2WO_6 and Eu^{3+} enhanced photocatalytic activity. This study highlights that *2*Eu-Bi_2WO_6 is a promising photocatalysts for environmental remediation under visible light.

ACKNOWLEDGMENTS

This research was supported by the Basic Science Research Program through the National Research Foundation of Korea (NRF) funded by the Ministry of Education (NRF-2017R1A2B4006388) and (NRF-2017R1D1A3B03035530).

SUPPORTING INFORMATION

Additional information as noted in the text. This information is available via the Internet at http://www.springer.com/chemistry/journal/11814.

REFERENCES

1. Y. Zhang, Y. Ma, Q. Liu, H. Jiang, Q. Wang, D. Qu and J. Shi, *Ceram. Int.*, **43**, 2598 (2017).
2. R. Van Deun, D. Ndagsi, J. Liu, I. Van Driessche, K. Van Hecke and A. M. Kaczmarek, *Dalton Trans.*, **44**, 15022 (2015).

3. L. S. Cavalcante, V. M. Longo, J. C. Sczancoski, M. A. P. Almeida, A. A. Batista, J. A. Varela, M. O. Orlandi, E. Longo and M. S. Li, *CrystEngComm.*, **14**, 853 (2012).
4. Y. Zhang, W. Gong, J. Yu, Z. Cheng and G. Ning, *RSC Adv.*, **6**, 30886 (2016).
5. F. Wang, W. Li, S. Gu, H. Li, H. Zhou and X. Wu, *RSC Adv.*, **5**, 89940 (2015).
6. N. K. Veldurthi, N. K. Eswar, S. A. Singh and G. Madras, *Catal. Sci. Technol.*, **8**, 1083 (2018).
7. Y. Zhou, P. Lv, W. Zhang, X. Meng, H. He, X. Zeng and X. Shen, *Appl. Surf. Sci.*, **457**, 925 (2018).
8. S. Jonjana, A. Phuruangrat, S. Thongtem and T. Thongtem, *Mater. Lett.*, **216**, 92 (2018).
9. H. Sun, Z. Tian, G. Zhou, J. Zhang and P. Li, *Appl. Surf. Sci.*, **469**, 125 (2019).
10. F. Xu, C. Xu, H. Chen, D. Wu, Z. Gao, X. Ma, Q. Zhang and K. Jiang, *J. Alloys Compd.*, **780**, 634 (2019).
11. M. Hojamberdiev, Z. C. Kadirova, E. Zahedi, D. Onna, M. Claudia Marchi, G. Zhu, N. Matsushita, M. Hasegawa, S. Aldabe Bilmes and K. Okada, *Arabian Journal of Chemistry* (2018), DOI:10.1016/j.arabjc.2018.07.014.
12. R. Chen, C. H. Hu, S. Wei, J. H. Xia, J. Cui and H. Y. Zhou, *Mater. Sci. Forum*, **743-744**, 560 (2013).
13. Y. Fu, C. Chang, P. Chen, X. Chu and L. Zhu, *J. Hazard. Mater.*, **254-255**, 185 (2013).
14. S. Yu, Y. Zhang, M. Li, X. Du and H. Huang, *Appl. Surf. Sci.*, **391**, 491 (2017).
15. X. Meng, M. Hao, J. Shi, Z. Cao, W. He, Y. Gao, J. Liu and Z. Li, *Adv. Powder Technol.*, **28**, 3247 (2017).
16. R. Radha, A. Srinivasan, P. Manimuthu and S. Balakumar, *J. Mater. Chem. C*, **3**, 10285 (2015).
17. Y. Bai, C. Bai and G. Mo, *Chem. Phys. Lett.*, **637**, 127 (2015).
18. H. Gu, L. Yu, J. Wang, M. Ni, T. Liu and F. Chen, *Spectrochim. Acta, Part A: Mol. Biomol. Spectrosc.*, **177**, 58 (2017).
19. C. Wang, Q. Zhu, C. Gu, X. Luo, C. Yu and M. Wu, *RSC Adv.*, **6**, 85852 (2016).
20. X. Xu, Y. Ge, B. Li, F. Fan and F. Wang, *Mater. Res. Bull.*, **59**, 329 (2014).
21. N. T. Kim Phuong, M.-w. Beak, B. T. Huy and Y.-I. Lee, *Chemosphere*, **146**, 51 (2016).
22. Y. R. Wang and W. Chu, *Appl. Catal. B: Environ.*, **123-124**, 151 (2012).
23. H. K. Singh, M. Saquib, M. M. Haque, M. Muneer and D. W. Bahnemann, *J. Mol. Catal. A: Chem.*, **264**, 66 (2007).
24. P. Dumrongrojthanath, A. Phuruangrat, S. Thongtem and T. Thongtem, *J. Ceram. Soc. Jpn.*, 126, 87 (2018).
25. X.-J. Zhang, *Ferroelectrics*, **514**, 34 (2017).
26. Y. Ma, Z. Chen, D. Qu and J. Shi, *Appl. Surf. Sci.*, **361**, 63 (2016).
27. X. Meng, H. Qin and Z. Zhang, *J. Colloid Interface Sci.*, **513**, 877 (2018).
28. B. T. Huy, C. T. B. Thao, V.-D. Dao, N. T. K. Phuong and Y.-I. Lee, *Adv. Mater. Interfaces*, **4**, 1700128 (2017).
29. N. T. M. Tho, B. T. Huy, D. N. N. Khanh, H. N. N. Ha, V. Q. Huy, N. T. T. Vy, D. M. Huy, D. P. Dat and N. T. K. Phuong, *Korean J. Chem. Eng.*, **35**, 2442 (2018).
30. J. M. Dostanić, D. R. Lončarević, P. T. Banković, O. G. Cvetković, D. M. Jovanović and D. Ž. Mijin, *J. Environ. Sci. Health, Part A*, **46**, 70 (2011).
31. N. Wang, L. Zhu, M. Wang, D. Wang and H. Tang, *Ultrason Sonochem.*, **17**, 78 (2010).
32. Y. L. Pang and A. Z. Abdullah, *Appl. Catal. B: Environ.*, **129**, 473 (2013).

Supporting Information

Enhanced performance in the photocatalytic degradation of 2,4,5-Trichlorophenoxyacetic acid over Eu-doped Bi_2WO_6 under visible light irradiation

Seong-Soo Lee[*,‡], Bui The Huy[*,,‡], Nguyen Thi Kim Phuong[***], Do Khanh Tung[****], and Yong-Ill Lee[*,†]**

*Department of Chemistry, Changwon National University, Changwon 51140, Korea
**Institute of Research & Development, Duy Tan University, 3 Quang Trung, Danang, Vietnam
***HoChiMinh City Institute of Resources Geography, VAST, 01 Mac Dinh Chi, Ho Chi Minh City, Vietnam
****Institute of Materials Science, VAST, 18 Hoang Quoc Viet, Cau Giay, Hanoi, Vietnam
(*Received 16 May 2019 • accepted 22 August 2019*)

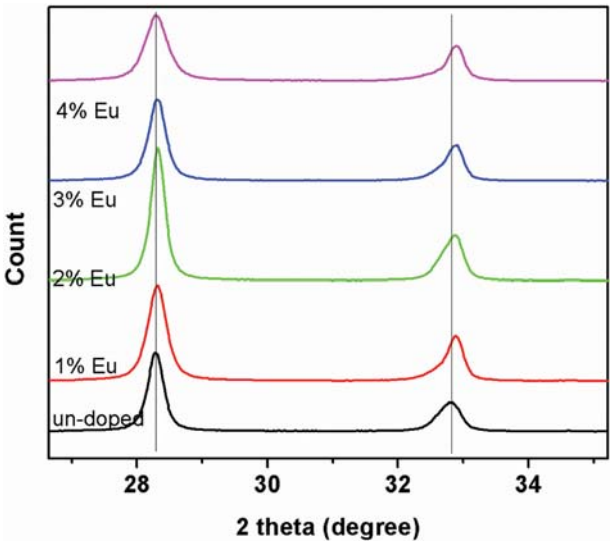

Fig. S1. Enlarged XRD patterns for selected 2θ ranges of the pristine and different doping level samples.

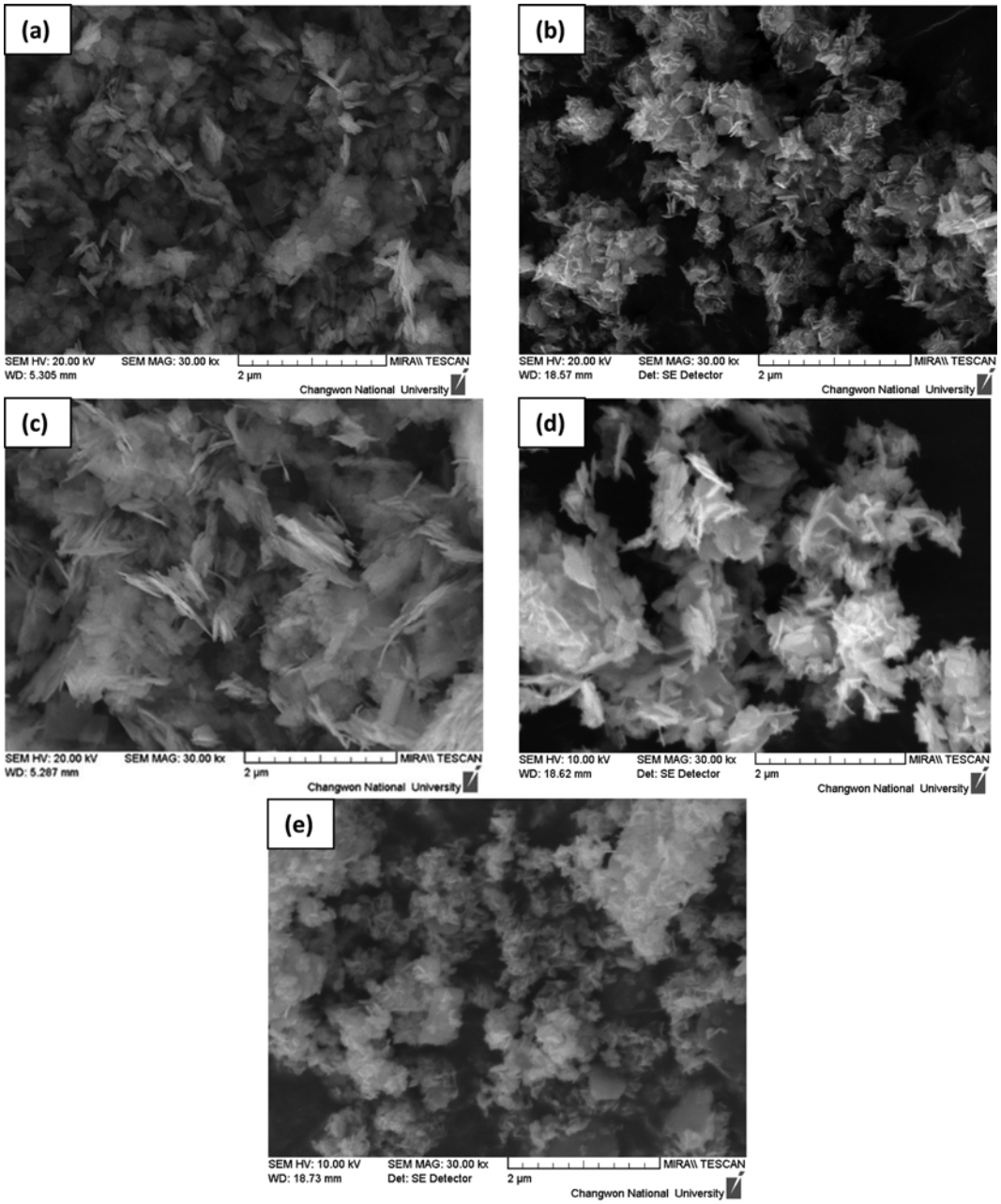

Fig. S2. SEM images of Bi_2WO_6 doped 0 (a), 1 (b), 2 (c), 3 (d), and 4% (e) Eu^{3+}.